

# Fluorescence yield and lifetime of isolated polydiacetylene chains: Evidence for a one-dimensional exciton band in a conjugated polymer

R. Lécuyer,<sup>1</sup> J. Berréhar,<sup>1</sup> J. D. Ganière,<sup>1,2</sup> C. Lapersonne-Meyer,<sup>1</sup> P. Lavallard,<sup>1</sup> and M. Schott<sup>1,\*</sup>

<sup>1</sup>*Groupe de Physique des Solides, UMR 7588 of CNRS, Universités Pierre et Marie Curie et Denis Diderot, Tour 23, 2 place Jussieu, 75251 Paris cedex 05, France*

<sup>2</sup>*IPEQ, FSB, Swiss Federal Institute of Technology, 1015 Lausanne, Suisse*

(Received 29 April 2002; revised manuscript received 5 July 2002; published 24 September 2002)

The fluorescence lifetime  $\tau$  and quantum yield  $\eta_f$  of isolated red polydiacetylene chains dispersed in their monomer single crystal matrix were measured between 10 and 100 K.  $\tau$  increases up to 120 ps at 40 K, then rapidly decreases at higher  $T$ .  $\eta_f$  is a continuously decreasing function of  $T$ . The radiative lifetime  $\tau_r$  is proportional to  $\sqrt{T}$  in the whole  $T$  range studied. This is the expected behavior for a purely one-dimensional system without localization, a behavior which is not usually observed even in semiconductor quantum wires. An order of magnitude of the exciton effective mass  $m^* \approx 0.3$  is inferred. The nonradiative lifetime  $\tau_{nr}$  is constant up to 50 K, then decreases exponentially, indicating the opening of a thermally activated decay channel.

DOI: 10.1103/PhysRevB.66.125205

PACS number(s): 78.67.Lt, 71.20.Rv, 71.35.-y, 78.55.-m

## I. INTRODUCTION

Polydiacetylene (PDA) chains in very low concentrations in their single crystal diacetylene monomer matrix are highly ordered one-dimensional (1D) noninteracting conjugated chains, and thus provide a good experimental model for studying the electronic properties of conjugated polymers. They are a very good approximation of an organic semiconducting quantum wire.

Bulk PDA's are known to exist in either of two electronic structures, so-called "red" and "blue" phases, showing intense excitonic absorptions near 2.4 and 2.0 eV, respectively. It was found recently<sup>1</sup> that in 3BCMU<sup>2</sup> monomer crystals, isolated chains of both types coexist. The majority population is of the "blue" type, with typical chain concentrations of  $10^{-5}$ – $10^{-4}$  in weight. The "red" chain concentration is about a thousand times smaller.

Both types of chains show exciton resonance fluorescence.<sup>1</sup> Thus emission from defects or self-trapped states can be ruled out. Blue chain fluorescence is extremely weak, with a quantum yield of  $\approx 10^{-4}$ .<sup>3</sup> Conversely, red chains have a high fluorescence quantum yield of  $0.30 \pm 0.05$  at 15 K, with more than 90% of the emission concentrated in a narrow (1.5–2 meV at 15 K) zero-phonon line at 543 nm, and the other 10% in a series of vibronic lines,<sup>3</sup> as shown in Fig. 1. The resonance character of the emission is demonstrated in Fig. 2: zero-phonon absorption and emission lines peak at the same energy and have similar widths. The sloping background in the absorption spectrum is due to absorption by blue chains also present in the crystal.

The very high dilution of red chains in 3BCMU crystals and their high fluorescence quantum yield in the zero-phonon line made a microphotoluminescence experiment possible. The recorded emission is indeed that of a single isolated chain. Its zero-phonon emission line is a single Lorentzian at all temperatures studied (6–60 K). It is a homogeneously broadened line with a linewidth increasing approximately linearly with  $T$  (350  $\mu$ eV at 6 K), indicating a

dephasing time of a few picoseconds or less.<sup>4</sup>

In this paper, the temperature dependence of the emission of a macroscopic ensemble of red chains is presented. Experimental results on the effective lifetime and fluorescence yield are presented and quantitatively interpreted in terms of an exciton band model. This gives experimental evidence for a 1D exciton band in ordered conjugated polymers, instead of the common description involving an exciton level.

## II. EXPERIMENTAL METHODS

3BCMU monomer crystals were grown from acetone or methyl-isobutylketone at 4 °C in the dark (typical dimensions  $5 \times 5 \times 0.1$  mm<sup>3</sup>). The PDA chain concentrations mentioned above are typical of such as-grown crystals; the experimental results reported here are independent of the exact concentrations.

The light source used for the study of the effective life-

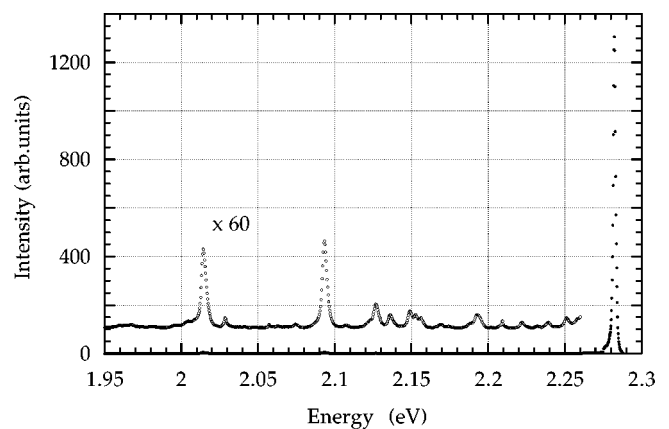


FIG. 1. Fluorescence emission spectrum of isolated red chains excited at 502 nm at 15 K. Full circles: zero phonon line at 2.28 eV. Open circles: vibronic emission spectrum; the two most intense vibronic lines correspond to the C=C stretch ( $D$  line at 2.09 eV) and C≡C stretch ( $T$  line at 2.015 eV).

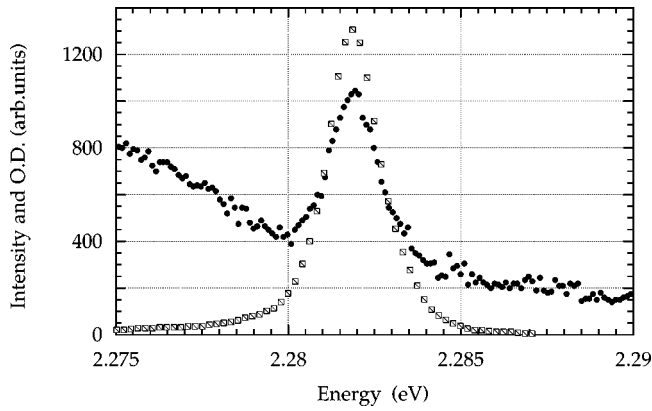


FIG. 2. Zero phonon line in emission (crossed squares) and in absorption (full circles).

time was a frequency-doubled Ti-sapphire laser. The temporal width of the pulse is typically smaller than 2 ps. The excitation beam was focused to a spot of  $\approx 100\text{-}\mu\text{m}$  diameter; in order to uniformly probe the excited sample region and to obtain a better scattered light rejection, the collected luminescence was spatially filtered in an intermediate image plane (magnification  $\times 4$ ) with a  $500\text{-}\mu\text{m}$ -diameter pinhole. A monochromator equipped with a 300 grooves/mm grating, and a streak camera with a nominal temporal resolution better than 4 ps, were used to analyze the luminescence. Taking into account all parameters including the residual jitter of the camera synchronization, the time and spectral resolutions were better than 15 ps and 1.5 nm, respectively. The excitation wavelength was chosen within the vibronic double bond stretch absorption band at circa 2.47 eV at low temperature.

This setup is almost the same as the one used in our previous study at 15 K.<sup>3</sup> However the lifetime reported here for the same temperature is larger. We became aware that the previously measured decay was slightly distorted by nonlinearities which made it faster at short times. In the present work, care was taken to eliminate these effects by working at low excitation power and small counting rates in the streak camera, always in the photon counting mode. The linearity of the detection was checked in the whole counting range. Absolute measurements of the fluorescence quantum yield at 15 and 40 K were performed using the experimental procedure described in details elsewhere.<sup>3</sup>

Since absolute yield measurements are time consuming and difficult in these crystals, the temperature dependence of the yield (relative values) was obtained following a different procedure. One must know the temperature dependence of its intensity for a constant number of absorbed photons. Since the red chains absorption can only be measured for the zero-phonon absorption line, excitation must be performed at its wavelength. But most of the emitted light is also in the resonance zero-phonon line at  $E_0$ , with the same polarization. Therefore, the determination of relative quantum yields involved several steps. First, the main (zero-phonon) absorption line was measured for several different samples between 10 and 80 K. This allows one to calculate the number of absorbed photons at all temperatures. Second, the temperature dependence of the intensity  $I_D$  of the vibronic double

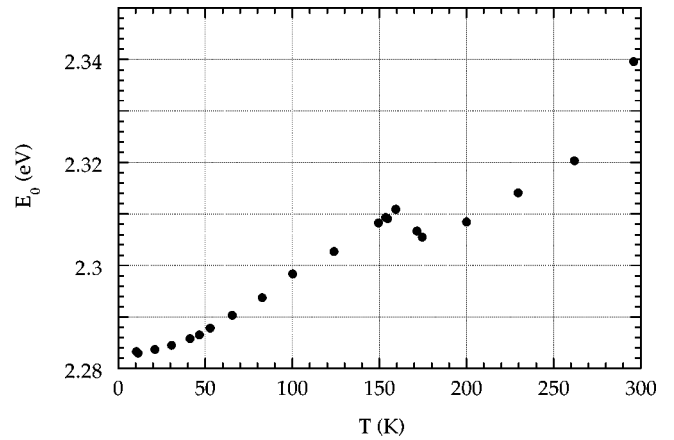


FIG. 3. Resonance emission energy  $E_0$  as function of temperature.

bond stretch line  $D$  excited, for all temperatures, at the energy of the main exciton absorption line  $E_0$  was measured between 10 and 80 K. Third, for the same range of temperatures, the ratio  $I_D/I_0$  of the  $D$  line and the zero phonon line was measured, exciting at all temperatures at  $E_0 + 20$  meV, corresponding to a vibronic line just above the zero-phonon line in the red chain absorption spectrum.<sup>3</sup> For all temperatures the experimental line shape can be fitted by Lorentzians above a weak and constant emission background. This allows one to determine analytically the spectrally integrated intensities. In that way, the temperature dependence of the dominant zero-phonon line  $I_0$  is evaluated for resonant excitation. These measurements allow us to determine the relative variation of the quantum yield in this range of temperatures. All these luminescence measurements were done using the dye Coumarin 540 pumped with the 488-nm line of an argon laser.

### III. TEMPERATURE DEPENDENCE OF THE EMISSION

#### A. Spectrum

Red chain fluorescence is intense enough to be seen at all temperatures up to room temperature. Figure 3 shows the resonance emission photon energy as a function of  $T$ . A discontinuity is seen near 150 K, where a first order transition of the monomer crystal is observed.<sup>5</sup> The present study is limited to the low temperature phase  $T < 150$  K. The exciton absorption linewidth for an ensemble of isolated red chains is constant  $\approx 3$  meV up to about 40 K, then increases linearly with  $T$  up to room temperature. Comparison with the single chain emission width<sup>4</sup> shows that the constant width below 40 K corresponds to inhomogeneous broadening while the line is homogeneously broadened above 40 K.

The emission spectrum keeps dominated by the zero-phonon line at all  $T$ , but the relative intensities of all vibronic emission lines relative to that of the zero-phonon one increase with  $T$ . Figure 4 shows, for instance, the  $T$  dependence of the ratio  $I_D/I_0$ , where  $I_D$  is the integrated intensity of the vibronic emission corresponding to the double bond stretching vibration, and  $I_0$  is the integrated intensity of the zero phonon line.

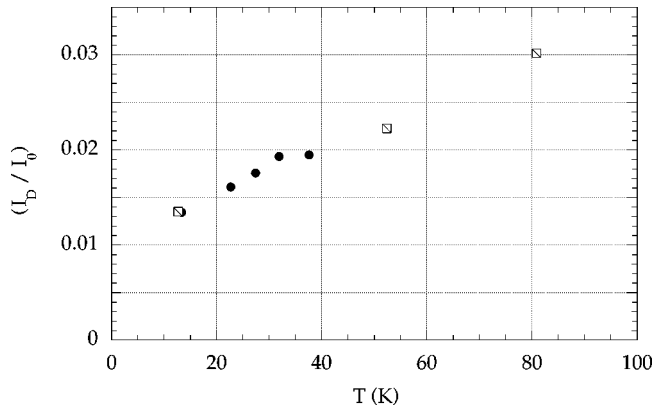


FIG. 4. Ratio  $(I_D/I_0)$  as a function of  $T$ .  $I_D$  is the integrated intensity of the vibronic emission corresponding to the double bond stretching vibration.  $I_0$  is the integrated intensity of the zero phonon line. Two different samples were used (full circles and crossed squares).

### B. Effective lifetime

A typical temporal variation of the fluorescence excited by a picosecond pulse at 500 nm is shown in Fig. 5, for  $T = 13$  K. The experimental rise of the emission signal is determined by the instrument response. So the actual emission risetime is much shorter than 1 ps. Moreover, there is no spectral shift of the emission during its rise and decay, and only resonance emission and its associated vibronic lines are observed. Therefore, the relaxation from the state initially prepared by absorption of the 500-nm photon occurs in the subpicosecond time scale. In the case of blue PDA chains, this time has been measured using the up-conversion method, and is less than 40 fs.<sup>6</sup> Such a time is typical of relaxation within the dense singlet manifold of large molecular systems.

At all temperatures studied, the decay is well fitted by a single exponential over more than 2 orders of magnitude. The corresponding decay time is determined with an accuracy of  $\pm 3\%$ .

The temperature dependence of  $\tau$  is shown in Fig. 6.  $\tau$

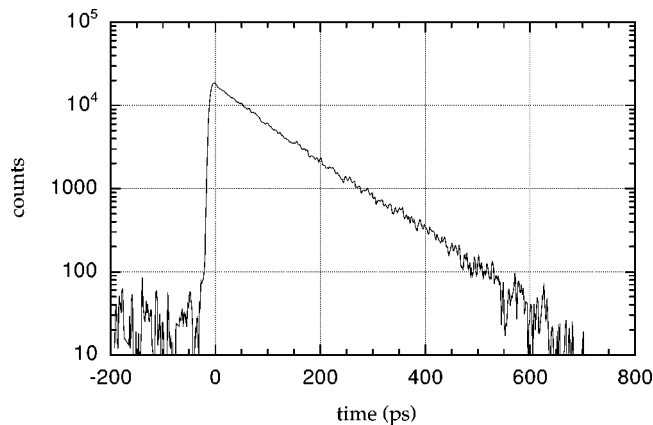


FIG. 5. Temporal variation of the fluorescence at 14 K. The whole decay is well fitted by a single exponential with  $\tau = 94$  ps, after subtraction of a small background.

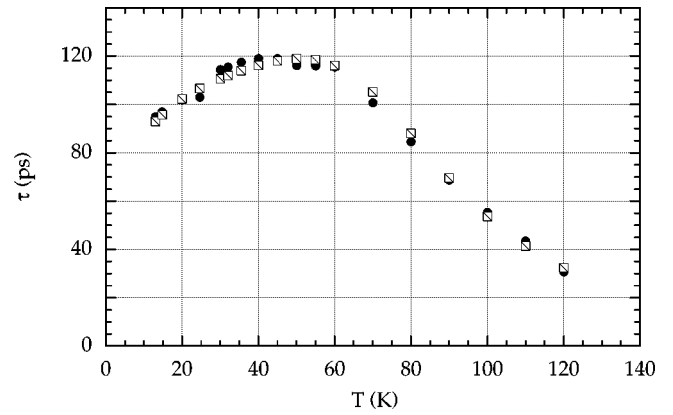


FIG. 6. Temperature dependence of the effective lifetime  $\tau$ . Full circles are experimental values and crossed squares are calculated (see Sec. IV D).

increases up to  $T \approx 40$  K, then decreases rapidly. Such a variation is not commonly observed in conjugated polymers. Understanding this unusual behavior is the basis of the present work.

### C. Fluorescence yield

Absolute values of the fluorescence quantum yield  $\eta_f$  were measured at two temperatures, 15 and 40 K:  $\eta_f(15 \text{ K}) = 0.30 \pm 0.05$  and  $\eta_f(40 \text{ K}) = 0.20 \pm 0.05$ . Relative values of  $\eta_f$  were derived by spectral integration of the vibronic double bond stretch line  $D$ , as described in Sec. III B above. The emission intensities at different temperatures are then scaled to an equal number of absorbed photons, including correction for the absorption of incident and emitted light by the blue chains. This scaling is only possible below  $\approx 70$  K, because at higher temperatures the red chain absorption becomes too broad, hence its intensity becomes too low compared to the blue chain absorption background. The total intensity emitted in all lines, and in particular the dominant zero-phonon line, is then calculated using the data of Fig. 4 for  $I_D/I_0$ . Only relative variations of  $\eta_f$  can be determined in this way since for instance the geometrical factor is not measured; care was taken, however, to keep all experimental conditions independent of temperature.

The relative variation with  $T$  is then scaled to the two measured absolute values, as shown in Fig. 7. It shows that  $\eta_f$  is a continuously decreasing function of  $T$ . The absolute values of  $\eta_f$  are uncertain to  $\pm 20\%$ , but the relative variations are more accurate (to  $\pm 5\%$ ).

## IV. INTERPRETATION AND DISCUSSION

### A. Implications for a two-level system

In the usual model of a single exciton level decaying to the ground state, the data for  $\tau(T)$  in Fig. 6 and for  $\eta_f(T)$  in Fig. 7 allow one to derive the radiative and nonradiative lifetimes  $\tau_r$  and  $\tau_{nr}$  at all  $T$ . The results are shown in Fig. 8 for  $\tau_r$  and Fig. 9 for  $\tau_{nr}$ . Here again, the relative variations of  $\tau_r$  and  $\tau_{nr}$  with  $T$  are accurate, but the uncertainty on  $\eta_f$  introduces a possible systematic error of  $\pm 20\%$ .

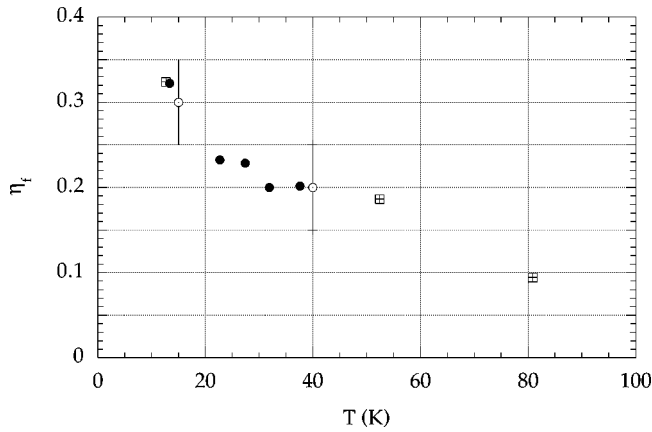


FIG. 7. Temperature dependence of the fluorescence yield  $\eta_f$ . Two samples were used to determine its relative variation with  $T$  (full circles and crossed squares). The open circles are the absolute values measured at 15 and 40 K with the evaluated uncertainties.

$\tau_r$  is found to increase between 10 and 40 K. However, the oscillator strength of the exciton transition can be measured by integrating the pure exciton absorption line—which is dominant in absorption as well. Figure 10 shows this integrated absorption in the range 10–70 K: it is constant or at most very weakly decreasing with  $T$ . The same behavior was found in all experiments. This is not consistent with the threefold increase of  $\tau_r$  shown in Fig. 6. We then conclude that a two level model cannot account for our data.

### B. Thermally accessible excited states

The existence of states lying above the  $B_u$  exciton level, thermally accessible from it and nonradiant to the ground state would explain that the effective lifetime increases with  $T$  while the fluorescence yield decreases. Two possibilities were considered.

(1) An  $A_g$  electronic excited state, nonradiant to the ground  $A_g$  state for symmetry reasons. The relaxation scheme of the exciton in blue PDA chains indicates the existence of at least one excited  $A_g$  state below the  $B_u$  exciton,<sup>7</sup>

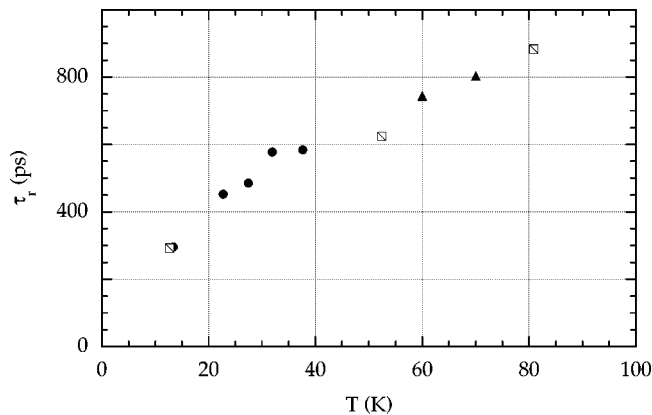


FIG. 8. Radiative lifetime  $\tau_r$  as a function of  $T$ . Two different samples were used (full circles and crossed squares). Two more points (full triangles) are calculated using the relation  $\tau_r = 80\sqrt{T}$  and the measured  $\tau(T)$  dependence.

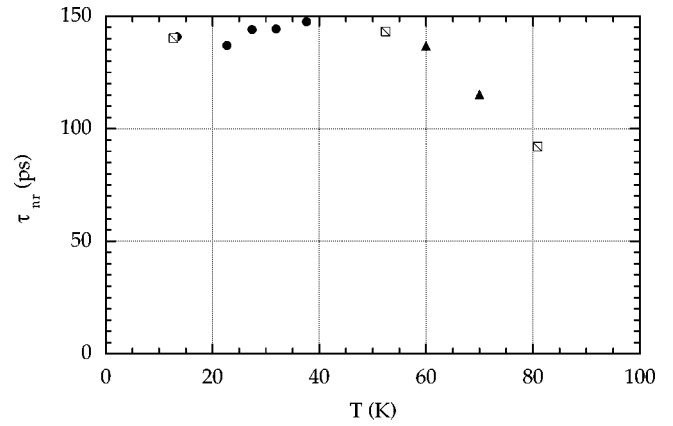


FIG. 9. Nonradiative lifetime  $\tau_{nr}$  as a function of  $T$  for two different samples. Same notations as in Fig. 8.

accounting for the very small fluorescence yield of blue chains<sup>1,3</sup> and their very short lifetime.<sup>6</sup> The high value of  $\eta_f$  in red chains indicates that this state is pushed above the  $B_u$  state; its actual energy is unknown, but might be close to the  $B_u$  energy. Another possibility would be that the unit cell in red chains contains two nontranslationally equivalent repeat units, hence a splitting of the exciton level, the lower level being radiatively coupled to the ground state.

(2) In a one-dimensional exciton band, the radiant states are those which momentum  $\mathbf{k}$  is equal to or smaller than the emitted photon momentum. All states with larger  $\mathbf{k}$  are non-radiant to the ground state due to the rule of conservation of the projection of momentum on the chain axis.

In both cases, these states may be radiatively coupled to vibrationally excited levels of the ground electronic state, but different behaviors are expected: In case 1, the  $B_u$  and  $A_g$  states will be coupled to different ground state vibrational levels,  $a_g$  and  $b_u$ , respectively. So vibronic emission lines are expected to appear upon increasing  $T$ . In case 2 on the other hand, all  $\mathbf{k}$  states of the exciton band can radiatively

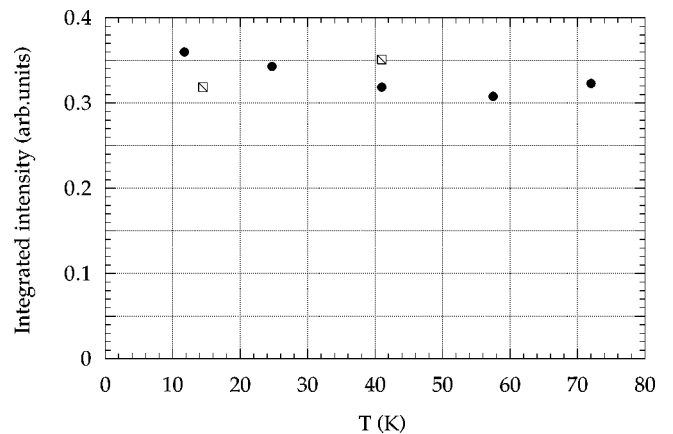


FIG. 10. Oscillator strength of the exciton transition measured by spectral integration of the zero phonon exciton absorption line as a function of  $T$ . A series of measurements on one sample is presented (full circles). Two points at 15 K and 41 K correspond to the values determined on a sample used for absolute measurements of the quantum yield at these temperatures (crossed squares).

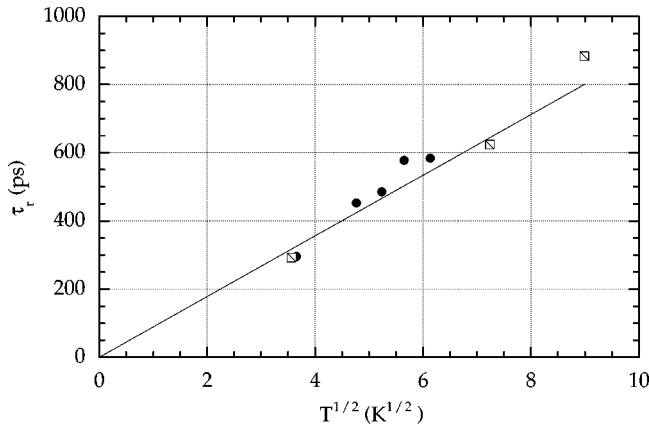


FIG. 11. Radiative lifetime  $\tau_r$  vs  $T^{1/2}$ . The data from two samples (full circles and crossed squares) fit a linear variation  $\tau_r = 90 T^{1/2}$  (thin line).

decay to the state of appropriate  $\mathbf{k}$  of the same vibrational band; hence an asymmetric broadening on the high energy side of all vibronic emission lines.

Experimentally, no new emission band appears, and the existing lines only show a temperature-dependent broadening on the high-energy side. However, it remains possible to fit the experimental line shape using two closely spaced Gaussians. So, although the exciton band model is clearly favored, the other model could not be unambiguously excluded. Any ambiguity is now removed by our recent microphotoluminescence experiments on a single red chain:<sup>8</sup> the vibronic lines remain single and show asymmetric broadening on their high energy side, which is quantitatively fitted using an exciton band model, with the predicted  $E^{-1/2}$  exciton density of states.

### C. Implications of the exciton band model

Our isolated PDA chains are geometrically one-dimensional objects. The theory for semiconducting quantum wires<sup>9</sup> is a natural frame for interpreting the present data.

This theory predicts that the temperature dependence of the radiative lifetime follows a  $T^{1/2}$  law. This is indeed the case in the whole  $T$  range studied, from 10 to 80 K, as shown in Fig. 11, where data from Fig. 8 replotted versus  $T^{1/2}$  fit a linear variation. Taking into account the uncertainty on the absolute value of  $\eta_f$ ,  $\tau_r = (80 \pm 20) \sqrt{T}$  picoseconds (with  $T$  in K). Using the mean absolute values for  $\eta_f$  as shown in Fig. 7 yields a prefactor of 90, while a direct fit of  $\tau(T)$  assuming a constant value of  $\tau_{nr}$  up to 50 K leads to a smaller value of about 70, suggesting that the actual fluorescence quantum yield is rather at the top of the error bar. It is important to note that, since the relative variations of  $\eta$  with temperature are known to a much better accuracy than the absolute values, the exponent of  $T$  is also determined to a good accuracy: calculation of the uncertainties leads to an exponent  $0.5 \pm 0.06$ .

Assuming the applicability of Citrin's calculation to the type of polymeric quantum wire studied here, his expression for the radiative lifetime,

$$\tau_r = \frac{2m_{ex}^* m_0 c_0}{2\alpha E_{ex}^0} \frac{1}{f_L} \sqrt{\frac{k_B T}{\pi E_1}} \quad (1)$$

can be used to estimate the exciton effective mass  $m_{ex}^*$  which is the only unknown quantity in the above expression. This expression corresponds to an infinite coherence length, so it only yields an upper limit of the exciton effective mass.  $E_{ex}^0 = 2.28$  eV is the exciton energy at  $\mathbf{k}=0$ , and its dependence on  $T$  is neglected in the  $T$  range considered.  $E_1$ , given by

$$E_1 = \frac{(\hbar \mathbf{k})^2}{2m_{ex}^* m_0}, \quad (2)$$

is the energy of the exciton band level which momentum  $\mathbf{k}_{ex}$  is equal to the emitted photon momentum.  $f_L$  is the exciton absorption oscillator strength per unit length of chain. It can be evaluated for blue chains by integrating the exciton absorption spectrum, yielding  $f \approx 0.3$  per repeat unit of the chain, and using the repeat unit length of  $5 \times 10^{-10}$  m. This yields  $f_L \approx 6 \times 10^8$  m<sup>-1</sup>. Assuming that blue and red chains have similar exciton oscillator strengths, a value  $m_{ex}^* \approx 0.3 \pm 0.1$  results from the relation  $\tau_r = (80 \pm 20) \sqrt{T}$ . This is of course only an order of magnitude estimate, which could be refined once a good measurement of the isolated red chains absorption spectrum becomes available. However, this estimate rests on the assumption of direct applicability of Citrin's calculation to a 1D conjugated polymer chain which is not proved at present.

This value of  $m_{ex}^*$  can be compared to what is known of the electron and hole effective masses, again in blue chains only. Angle-resolved ultraviolet photoemission spectroscopy measurement of the valence-band dispersion yields  $m_h^* \approx 0.1$ .<sup>10</sup> Electroabsorption of isolated blue chains shows a strong Franz-Keldysh effect from which a reduced mass  $(m_e^{*-1} + m_h^{*-1})^{-1} \approx 0.05$  is deduced; hence  $m_e^* \approx 0.1$  as well.<sup>11</sup> Thus  $m_{ex}^*$  is approximately equal to the sum of the carrier effective masses, as expected in semiconductor theory.

It was shown in Fig. 4 that the integrated intensity ratio  $I_D/I_0$  increases with  $T$ . This is indeed expected since any  $\mathbf{k} \neq 0$  state is radiatively coupled to the state of same  $\mathbf{k}$  in the vibrational  $D$  band of the ground state: exciton states of all  $\mathbf{k}$  thus contribute to the total  $D$  line emission, but only those close to  $\mathbf{k}=0$  contribute to the zero phonon emission. Assuming that the emission probabilities to states of the  $D$  vibrational band are independent of the exciton  $\mathbf{k}$  value, the  $I_D/I_0$  ratio is also predicted to follow a  $T^{1/2}$  law. As shown in Fig. 12, our data fit such a law.

The observation of an exciton density of states proportional to  $E^{-1/2}$  in an isolated PDA red chain,<sup>8</sup> with its consequences on both the  $T$  dependences of  $\tau_r$  and the ratio  $I_D/I_0$  reported here, indicate that the emitting state is not a localized state. This is not commonly observed in semiconducting quantum wires.<sup>12</sup> Lateral size variation is claimed to be a major cause of localization in semiconductor quantum wires. No such variation exists in the polymer chains studied here, which consist of a single linear chain of Carbon atoms.

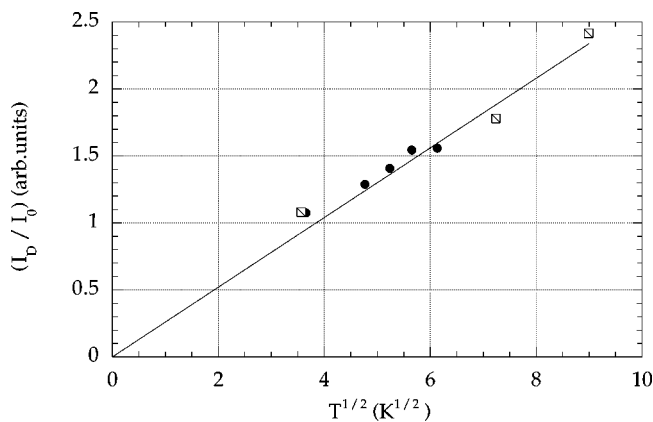


FIG. 12. Ratio  $(I_D/I_0)$  vs  $T^{1/2}$ . The data from two samples (full circles and crossed squares) fit a  $T^{1/2}$  law (thin line).

#### D. Nonradiative processes

From Fig. 9, the nonradiative lifetime is independent of  $T$  up to about 60 K,  $\tau_{nr} = 150 \pm 15$  ps. This is a  $\mathbf{k}$ -independent nonradiative channel, since at 60 K a significant fraction of the exciton population is already in  $\mathbf{k} \neq 0$  states. Above 60 K the nonradiative lifetime  $\tau_{nr}$  starts decreasing rapidly (Fig. 9), suggesting that another, thermally activated, channel takes over. This decrease can be fitted by an exponential temperature dependence with an activation energy  $\approx 38$  meV and a preexponential factor of a few  $10^{11} \text{ s}^{-1}$ . This is shown in Fig. 6 where the fit is compared to the experimental data. The fit was computed assuming that the  $T^{1/2}$  variation of  $\tau_r$ , with  $T$  determined above, and the  $T$  independent contribution

to  $\tau_{nr}$ , can both be extrapolated to temperatures higher than 50 K. The prefactor to the  $T^{1/2}$  variation and the parameters of the exponential contribution to  $\tau_{nr}$  were then fitted.

The nature of these non radiative processes is not known. One usually considers internal conversion to the ground state and intersystem crossing to the triplet manifold. However, another process may exist in the PDA: in blue PDA chains, singlet exciton fission into a triplet pair is a very efficient process, starting  $\approx 0.12$  eV above the singlet  $B_u$  exciton energy.<sup>13</sup> A similar situation in red chains might account for the thermally activated nonradiative channel. Further experimental study of this problem is planned.

#### V. CONCLUSION

In conclusion, we have presented experimental results showing that the red PDA chains' fluorescence quantum yield continuously decreases as  $T$  increases, while the effective luminescence lifetime increases up to 40 K, then decreases. These results are quantitatively explained using an exciton band model. In particular, the radiative lifetime follows the  $T^{1/2}$  law expected for a perfect 1D system. This behavior is not observed in other so-called 1D systems such as semiconductor quantum wires<sup>12</sup> or  $J$  aggregates of some organic dyes.<sup>14</sup> From the absolute values of  $\tau_r$ , an exciton effective mass  $m_{ex}^* \approx 0.3$  was estimated, close to the sum of electron and hole effective masses.

Two nonradiative processes compete with radiative decay. At low temperature a constant,  $\mathbf{k}$ -independent process, is observed. A thermally activated process takes over above  $\approx 50$  K.

\*Corresponding author. Email address: schott@gps.jussieu.fr

<sup>1</sup>R. Lécuyer, J. Berréhar, C. Lapersonne-Meyer, and M. Schott, Phys. Rev. Lett. **80**, 4068 (1998).

<sup>2</sup>The general formula of PDA is  $(=CR-C\equiv C-CR'=)_n$ . In 3BCMU, the side groups  $R$  and  $R'$  are identical, with a molecular formula  $-(CH_2)_3OCONHCH_2COOC_4H_9$ .

<sup>3</sup>R. Lécuyer, J. Berréhar, C. Lapersonne-Meyer, M. Schott, and J.-D. Ganière, Chem. Phys. Lett. **314**, 255 (1999).

<sup>4</sup>T. Guillet, J. Berréhar, R. Grousson, J. Kovensky, C. Lapersonne-Meyer, M. Schott, and V. Voliotis, Phys. Rev. Lett. **87**, 087401 (2001).

<sup>5</sup>S. Spagnoli *et al.*, (unpublished).

<sup>6</sup>S. Haacke, J. Berréhar, C. Lapersonne-Meyer, and M. Schott, Chem. Phys. Lett. **308**, 363 (1999).

<sup>7</sup>B. Kraabel, M. Joffre, C. Lapersonne-Meyer, and M. Schott,

Phys. Rev. B **58**, 15 779 (1998).

<sup>8</sup>F. Dubin, J. Berréhar, R. Grousson, T. Guillet, C. Lapersonne-Meyer, M. Schott, and V. Voliotis, Phys. Rev. B (to be published).

<sup>9</sup>D.S. Citrin, Phys. Rev. Lett. **69**, 3393 (1992).

<sup>10</sup>W.R. Salaneck, M. Fahlman, C. Lapersonne-Meyer, J.-L. Fave, M. Schott, M. Lögdlund, and J.-L. Brédas, Synth. Met. **67**, 309 (1994).

<sup>11</sup>A. Horvath, G. Weiser, C. Lapersonne-Meyer, M. Schott, and S. Spagnoli, Phys. Rev. B **53**, 13507 (1996).

<sup>12</sup>See, for instance D.Y. Oberli, M.-A. Dupertuis, F. Reinhardt, and E. Kapon, Phys. Rev. B **59**, 2910 (1999)

<sup>13</sup>B. Kraabel, D. Hulin, C. Aslangul, C. Lapersonne-Meyer, and M. Schott, Chem. Phys. **227**, 83 (1998).

<sup>14</sup>E.O. Potma and D.A. Wiersma, J. Chem. Phys. **108**, 4894 (1998).